How to cite: *Angew. Chem. Int. Ed.* **2023**, *62*, e202307165
doi.org/10.1002/anie.202307165

VIP **Natural Products** *Very Important Paper*

Structure Elucidation of the First Sex-Inducing Pheromone of a Diatom

*Franziska A. Klapper, Christine Kiel, Peter Bellstedt, Wim Vyverman, and Georg Pohnert**

Abstract: Diatoms are abundant unicellular microalgae, responsible for ≈20 % of global photosynthetic CO_2 fixation. Nevertheless, we know little about fundamental aspects of their biology, such as their sexual reproduction. Pheromone-mediated chemical communication is crucial for successful mating. An attraction pheromone was identified in the diatom *Seminavis robusta*, but metabolites priming cells for sex and synchronizing search and mating behavior remained elusive. These sex-inducing pheromones (SIP) induce cell cycle arrest and trigger the production of the attraction pheromone. Here we describe the challenging structure elucidation of an *S. robusta* SIP. Guided by metabolomics, a candidate metabolite was identified and elucidated by labeling experiments, NMR, ESI MS^n analyses, and chemical transformations. The use of negative ion mode MS was essential to decipher the unprecedented hydroxyproline and β-sulfated aspartate-containing cyclic heptapeptide that acts in femtomolar concentrations.

Diatoms are unicellular photosynthetic microalgae that contribute massively to the primary production in the oceans.[1] They often dominate phytoplankton and biofilm communities and form the base of the marine food chain. These unicellular algae predominantly reproduce by asexual mitotic divisions. Due to their biomineralized cell walls made out of silica, cell divisions lead to a decrease in cell size in many species.[2] When diatoms reach a species-specific sexual size threshold, they can switch to short episodes of sexual reproduction resulting in cell size restoration.[3,4] Such events are under the control of pheromones that ensure synchronization and support the mate-finding process of the motile cells.[5,6] Elucidation of these water-born signaling cues is challenging due to the extremely low active concentrations and the only episodic observation of sexuality that is hard to control under laboratory conditions.

The benthic diatom *Seminavis robusta* was established as a model to study sexuality in diatoms.[7–9] In synchronized cultures, comparative metabolomics enabled the identification of three candidate metabolites for pheromones that are only produced by sexually mature cells.[10,11] An attraction pheromone was identified as the diketopiperazine dimer of L-proline (diproline).[10] It is released in relatively high amounts by the calling mating type mt^- and guides cells of the opposite, attracted mating type (mt^+) to their partners (Figure 1). Diproline is only produced by mt^- cells when a potential mt^+ partner is signaling its presence by the sex inducing pheromone SIP^+.[10] The SIP^+ has a dual function in triggering pheromone release and arresting the cell cycle of the partner cell, thereby increasing the chances for successful mating. A third pheromone is the synchronizing SIP^- produced by mt^- cells, which signals the presence and availability for mating and induces diproline receptor formation in mt^+ cells. Despite substantial efforts, the SIP candidates were hitherto only characterized by their masses because they are produced in quantities far below the amounts required for common NMR analysis.[11] Here, we report the challenging elucidation of SIP^+ using a combination of sophisticated analytical and microbiological methods.

Comparative mass spectrometry based metabolomics of sexual and non-sexual mt^+ cells revealed the SIP^+-candidate

[*] F. A. Klapper, Dr. C. Kiel, Prof. Dr. G. Pohnert
Institute for Inorganic and Analytical Chemistry, Bioorganic Analytics, Friedrich Schiller University Jena
Lessingstrasse 8, 07743 Jena (Germany)
E-mail: georg.pohnert@uni-jena.de

Dr. C. Kiel
Department of Plankton and Microbial Ecology, Leibniz Institute of Freshwater Ecology and Inland Fisheries
Zur alten Fischerhütte 2, 16775 Stechlin (Germany)

Dr. P. Bellstedt
Institute of Organic and Macromolecular Chemistry, Friedrich Schiller University Jena
Humboldtstraße 10, 07743 Jena (Germany)
and
Institute of Clinical Chemistry, University of Zurich & University Hospital
Rämistrasse 100, 8091 Zürich (Switzerland)

Prof. Dr. W. Vyverman
Laboratory of Protistology and Aquatic Ecology, Department of Biology
Ghent University
Krijgslaan 281 S8, 9000 Ghent, Belgium

Prof. Dr. G. Pohnert
Max Planck Institute for Chemical Ecology
Hans-Knöll-Straße 8, 07745 Jena (Germany)

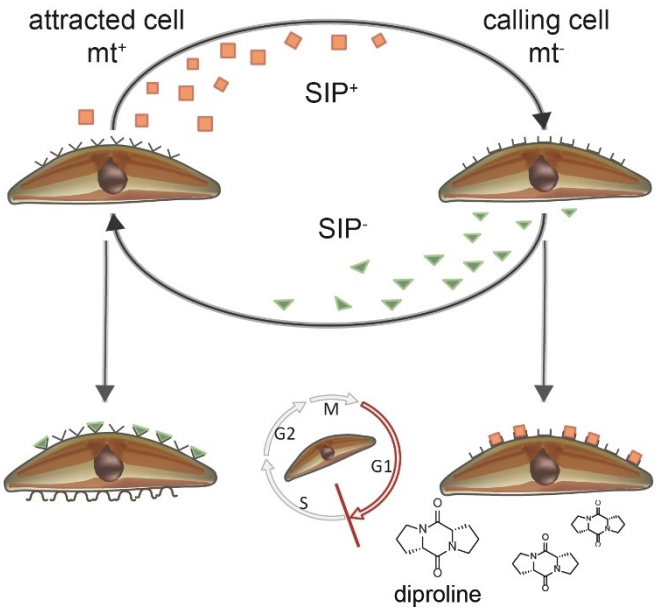

Figure 1. Pheromone system of *Seminavis robusta*. Once mt^+ cells reach a sexual size threshold they exude the SIP^+ which triggers the production of the attraction pheromone diproline in the opposite mating type. SIP^- of mt^- cells induces receptor formation for diproline in mt^+ cells. Both SIPs arrest the cell cycle of the opposed mating type in G1 phase to enable the transition to meiosis.

with a mass of $[M-H]^-$ *m/z* 842.2042 Da that was always and exclusively present in the medium of sexual cells that were below the sexual size threshold. Partially purified fractions from mt^+ culture medium extract containing this metabolite were active in bioassays monitoring the induced production of the attraction pheromone diproline.[11] Fractions lacking the compound were always inactive. After cultivation, extraction, and purification of several hundreds of liters of culture supernatant we obtained minute amounts of the pheromone insufficient for NMR analysis. Due to low quantities of SIP^+, structure elucidation required in-depth high resolution ESI MS/MS analysis and sophisticated NMR measurements using natural isotope and stable isotope enriched samples.

In negative ion mode MS, we identified an isotopic pattern characteristic of a molecule containing three sulfur atoms, but the molecular formula remained ambiguous. Successful determination of the elemental composition was only possible after labeling experiments (Figure S2A). Cells of *S. robusta* almost quantitatively incorporated ^{15}N after two cycles of culturing in artificial seawater containing $^{15}NO_3^-$ as single nitrogen source, and the mass of fully labeled SIP^+ shifted by 6.9742 Da corresponding to seven labeled nitrogen atoms present in the molecule. Using this information, the molecular formula of SIP^+ was determined based on $[M-H]^-$ *m/z* 842.2042 Da as $C_{29}H_{45}N_7O_{16}S_3$ (calculated 842.2012, Δm 3.6 ppm), which requires eleven double bond equivalents. For clarity, the detailed fragmentation analysis is described first, followed by NMR and further analyses.

Collision induced dissociation (CID) spectra with low normalized collision energy (NCE) were dominated by the fragment $[M-H-SO_3]^-$ resulting from the loss of SO_3.[11] At 25 NCE, two fragments readily form (dominant ions *m/z* 374.1205 and *m/z* 387.1167), explaining the lack of fragments in the range *m/z* 400–600 (Figure 2A). Analysing these fragments of ^{15}N labeled SIP^+ (Figure S4) resulted in the assignment of $C_{14}H_{21}N_3O_9$ and $C_{15}H_{24}N_4O_4S_2$ which combined correspond to the desulfated metabolite. A detailed analysis of minor fragments revealed an ion of *m/z* 454.0774, that gave a first indication that the sulfate is positioned in y_3^- (Figure 2A). The dominant ions could be subsequently identified as y_3^- $-SO_3$ and b_4^- of a deprotonated peptide formed by α- and β-cleavage, respectively (Figure 3).[12] Thereby, y- and b-fragments of peptides are formed by backbone cleavages at the C(O)N structural motives and refer to either *C*-terminal (y) or *N*-terminal (b) fragments.[13] Later this fragmentation could be explained by a cleavage of the amide bond of (hydroxy)proline that is preferred in peptides.[14]

The loss of multiple amino acid side chains and the subsequent loss of the remaining *C*-terminal peptide backbone substructure entity C_2H_3NO suggested that SIP^+ is of peptidic nature, which was confirmed by NMR analysis of labeled SIP^+ (see below). Negative ion mode MS/MS did not result in dominant fragment ions typical for peptides fragmented in positive ion mode, but the neutral losses of the amino acid side chains allowed the assignment of sulfur containing amino acids (Figure 2A).[15] Loss of H_2S (Δm 33.9878 Da) as well as H_2S_2 (Δm 65.9597 Da) were indicative for two cysteine residues that form a disulfide moiety.[16] This finding was further confirmed by the reduction of SIP^+ with dithiothreitol, which resulted in a mass of $[M-H+2H]^-$ and a reduced retention time upon reversed phase chromatography due to increased polarity (Figure S6).

Supported by our NMR analysis (see below), we correlated the neutral loss of $C_2H_2O_3$ (CO_2+CH_2O) derived from the $[M-H-SO_3]^-$ fragment (Δm 74.0003 Da) with the presence of an unusual β-hydroxy aspartic acid residue. β-OH-Asp (Hya) is found in siderophores produced by marine bacteria[17,18] but not yet described in any natural product from algae.

At 35 NCE several smaller fragments were observed that required MS^3 analysis to assign them to either y_3^-–SO_3 or b_4^- of the peptide (Figure 2B, Figure S5). Using in source fragmentation with subsequent CID, a repeated loss of hydroxyproline (Hyp, Δm 113.0478 Da) could be assigned to the y-series. The y_1^-–SO_3 fragment *m/z* 148.0253 ($C_4H_6NO_5^-$) confirms the amino acid Hya at the *C*-terminus of the peptide (Figure 3). The fragment $b_4 - H_2S_2$ was indicative of the two S–S-connected cysteine residues as part of b_4^-.

Further amino acids were identified from CID spectra acquired in positive ion mode, typically showing iminium ions. Two iminium ions of *m/z* 86 that differ in less than 0.04 Da could be assigned to Leu and Hyp, respectively (Figure 4A). The fragments *m/z* 68.0496 and *m/z* 114.0550 could also be assigned to hydroxyproline, verifying the presence of this amino acid residue in y_3. The linear part y_3

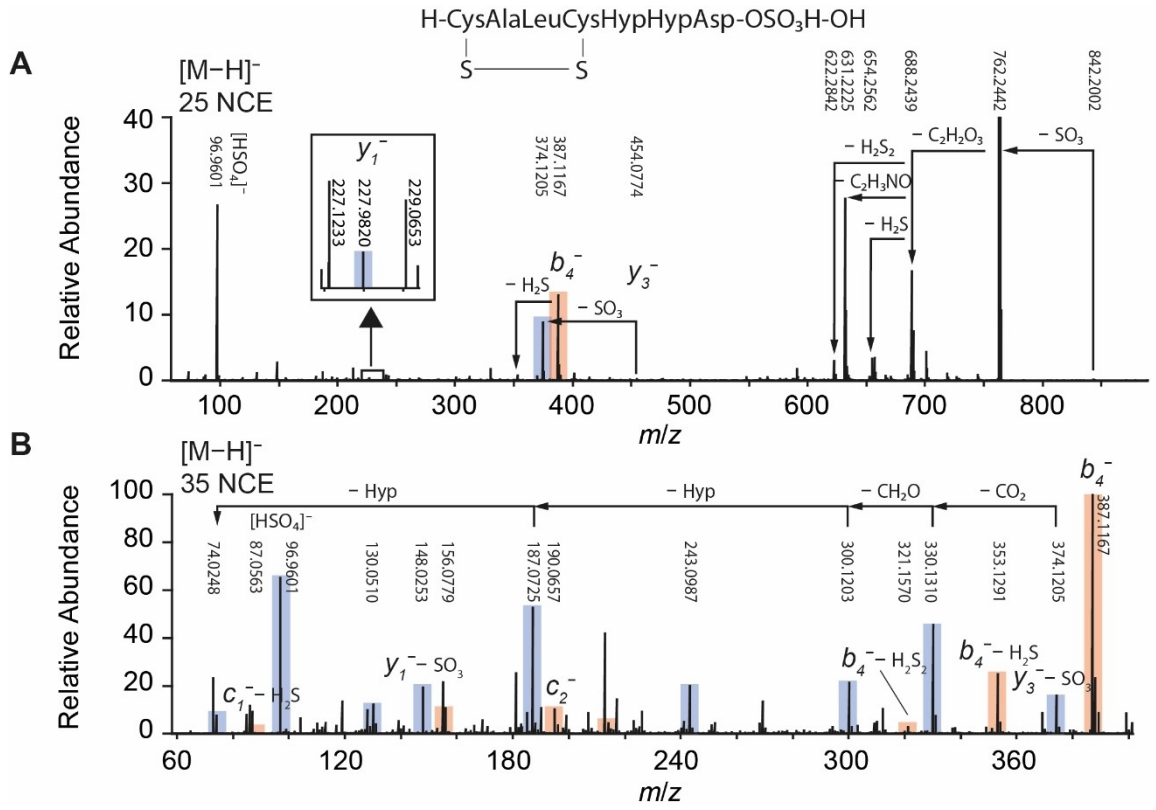

Figure 2. ESI MS/MS spectra of SIP^+ using different normalized collision energy (NCE). (A) In negative ion mode, the molecule cleaves into two parts, a linear one containing a sulfate group (blue) and a cyclic one bearing a disulfide bridge (orange). The box shows y_1^- magnified 100-fold. (B) Increased collision energy yields smaller fragments that were assigned to be derived from b_4^- (orange) or y_3^-–SO_3 (blue) based on MS^3 measurements.

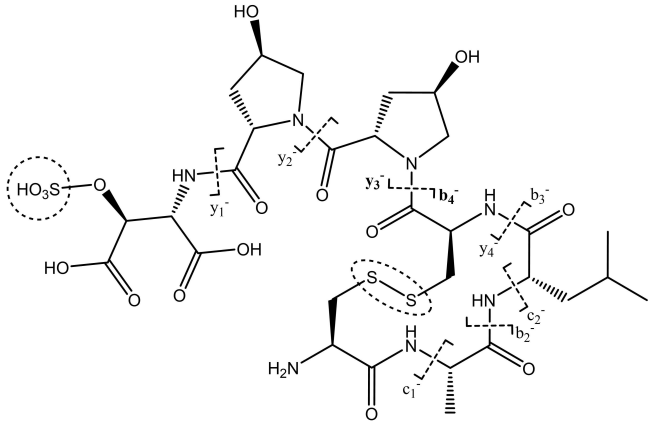

Figure 3. CID-MS fragmentation analysis of SIP^+ in negative ion mode.

of the peptide resulted in the expected *y*-series, and corresponded to the sequence Hya–Hyp–Hyp.

Eventually, fragmentation of reduced SIP^+ revealed the b_4 fragment *m*/*z* 391.1474 of the reduced, 2 Da heavier precursor ion and the iminium ion of Cys confirming two Cys residues to form a disulfide bridge in the cyclic substructure b_4 of SIP^+ (Figure 4B). Further, the b-series indicated an additional Ala (b2 in Figure 4B), which could be confirmed by NMR analysis (Figure 5). The fragment ion *m*/*z* 217.0644 supported that the two neighboured amino acids Hyp3–Cys4 connect the linear and the cyclic part of the peptide.

To support the initial MS-assignments, we utilized NMR for further structure elucidation. However, the extraction of more than 200 L medium did not yield sufficient amounts of SIP^+ for NMR analysis. We therefore had to revert to isotope enrichment experiments. A cultivation of ≈80 L of *S. robusta* was performed with ^{13}C carbonate and ^{15}N nitrate-enriched medium to increase sensitivity for NMR analysis. A 30 % degree of ^{13}C-labeling proved to increase sensitivity without complicating the signals due to C–C coupling (Figure S2 B). This was achieved by culturing in culture vessels that allowed exchange with atmospheric $^{12}CO_2$. MS^2 data of labeled SIP^+ revealed a uniform distribution of incorporated ^{13}C carbon in the respective fragments (Figure S3). ^{15}N-enrichment in SIP^+ was nearly quantitative. After several purification steps including solid phase extraction, size exclusion chromatography, and reversed phase chromatography we obtained less than 200 µg of SIP^+, emphasizing the challenge of SIP^+ structure elucidation. NMR spectroscopy of SIP^+ in D_2O on 500 MHz and 600 MHz instruments equipped with cryoprobes allowed further characterization of the molecule. ^1H NMR signal intensity was below the signal to noise threshold required for evaluation, due to coupling with enriched ^{13}C and ^{15}N

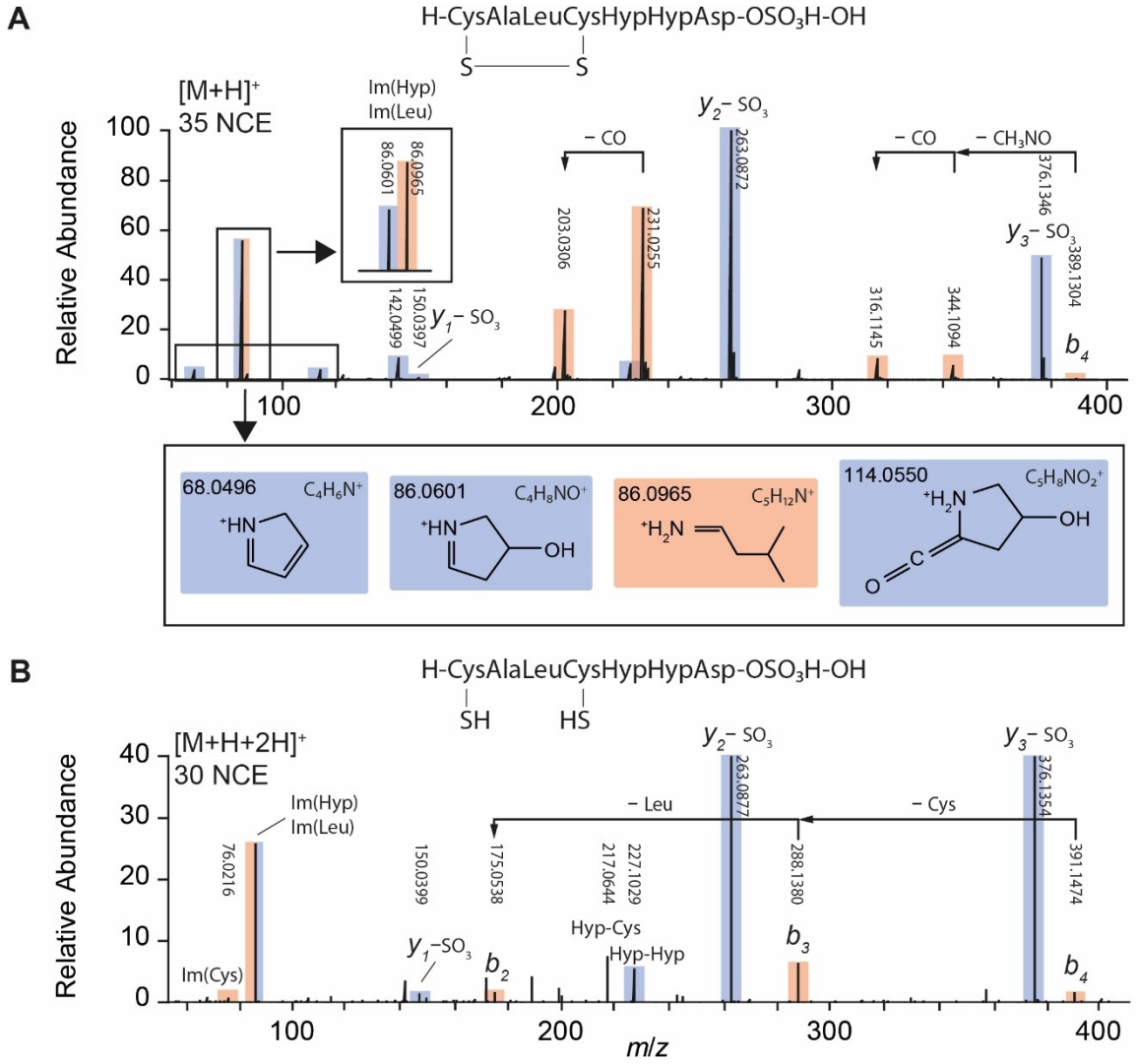

Figure 4. ESI CID spectra of native and reduced SIP^+ conducted in positive ion mode. (A) The fragmentation of b_4 (orange) and y_3–SO_3 (blue) fragment ions of SIP^+ between *m/z* 60 to 400 is shown and verified by MS^2 of the respective fragments. At high collision energies iminium ions (Im) of amino acids are detected as well as the y-series. The boxes indicate key fragments in the range of *m/z* 60–120 and their assigned structures. (B) Fragmentation of reduced SIP^+ reveals the typical b-series.

nuclei (Figure S8). Due to the low amounts of the active metabolite trace impurities introduced during purification were detected, but these did not contribute to activity (Figure S8). Only 10 out of 29 carbons could be detected by 1D-^{13}C NMR (Figure S9). However, two-dimensional NMR experiments provided crucial information required to conclude the structure of SIP^+. ^{1}H,^{15}N HMBC data verified seven nitrogen atoms in the pheromone corresponding to six amides and the *N*-terminal amino moiety of the peptide (Figure S10). ^{1}H,^{13}C HMBC revealed resonances for six peptide carbonyl carbons in the region of δ_C 178–173 ppm and two additional carbonyl carbons of the *C*-terminal β-hydroxy aspartic acid (Hya) (Figure S11). In accordance with the sum formula, the ^{1}H,^{13}C HSQC-DEPT spectra (Figure S12) showed signals for the remaining 21 sp^3 carbon atoms including several methine carbons in the range of δ_C 62–54 ppm, corresponding to the C_α of amino acids (Table S2).

Although the two Cys–C_α showed only weak signals (δ_C 57.4 ppm and 55.3 ppm), carbon atoms of all seven amino acids could be assigned based on HMBCs and ^{1}H,^{13}C H2BC[19] cross peaks (Figure S11, S13). Seven individual spin systems were detected by ^{1}H,^{1}H TOCSY (Figure 5, Figure S14). Only the ^{13}C signal at 72.7 ppm (δ_H 4.64 ppm, ^{1}H,^{13}C HSQC) represented two methine carbons of the Hyp side chains that were not resolved and could therefore not be differentiated. However, the downfield shift of these methine carbons (δ_C 72.7 ppm) supported the hydroxylation of both carbon atoms in the amino acid side chains. Its assignment to Hyp–C8/13 is based on the direct neighborhood to Hyp–C7/12 (δ_C 39.6 ppm/38.9 ppm) and Hyp–C9/14 (δ_C 57.9 ppm/57.1 ppm) based on the H2BC cross peak from Hyp–**H**7/12 (δ_H 2.4 ppm) and Hyp–**H**9/14 (δ_H 3.8 ppm) to

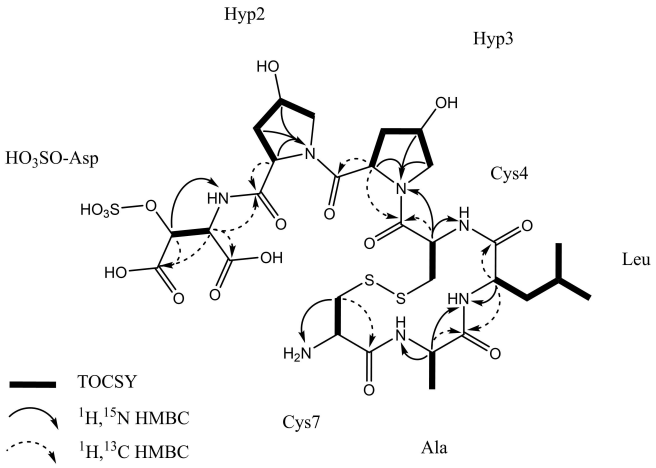

Figure 5. Key correlations within the individual amino acid residues (TOCSY) and HMBC experiments for SIP^+.

Hyp–**C**8/13. Moreover, the intramolecular disulfide bridge was evident from the downfield shift of the Cys–C17/29 (δ_C 38 ppm/44 ppm).[20] These structural features were consistent with the 11 double bond equivalents determined from the SIP^+ sum formula. Finally, the downfield chemical shifts of the oxymethine (δ_C 81.1 ppm, δ_H 5.0 ppm) disclosed the sulfated Hya.[21] The specific search for the modified Hya in MS data also revealed the fragment ion peak at *m/z* 227.9820 ($C_4H_6NO_8S$, Figure 2A box, y_1^-) confirming the β-sulfated aspartic acid. While sulfated threonine and serine are common,[22] this is the first example where a β-sulfated aspartate is found in a peptide. Hitherto only one example of a sulfated asparagine was reported from sponges.[23] Sulfation of plant peptide hormones is a mechanism for the activation of peptides or for specification of the peptide for receptor recognition.[24] Whether such a regulation is also involved in diatom sex-pheromone activation is not known, but we did not find any indication of a desulfated SIP^+ in LC/MS.

From $^1H,^{13}C$ and $^1H,^{15}N$ HMBC NMR, the peptide linkage of Hyp3–Cys4 between the linear and the cyclic part of SIP^+ was verified by the correlation of Hyp3–**H**11 (δ_H 4.9 ppm) with Cys4–**C**O and of Cys4–**H**16 (δ_H 4.87 ppm) with Hyp3–**N**, respectively. The placement of Ala next to Leu within the cyclic part of the molecule was supported analogously by correlations from the Leu–**H**19 (δ_H 4.45 ppm) to Ala–**C**O and confirmed by the cross peak from Ala–**H**25 (δ_H 4.3 ppm) to Leu–**N** (Figure S10, S11), respectively. The correlation from Cys–**H**29 (δ_H 3.35 ppm) to Cys–**N** (δ_N 31.3 ppm) was indicative of Cys at the *N*-terminus of the peptide (Figure S10). Given the dipeptide motif H–Ala–Leu–OH, an *N*-terminal Cys7 and the linkage Hyp3–Cys4, the primary sequence of SIP^+ was confirmed to be (HO_3SO)–Hya Hyp2 Hyp3 Cys4 Leu Ala Cys7.

To identify the absolute configuration of SIP^+, its ten stereogenic centers were addressed by Marfey's analysis.[25] Less than 100 µg of SIP^+ were hydrolyzed with 6 N HCl, which also cleaved the sulfate ester, to give the free amino acids. Amino acid standards, racemic *threo* and *erythro* β-OH-Asp as well as the hydrolyzed SIP^+ sample were derivatized with 1-fluoro-2–4-dinitrophenyl-5-L-alanine amide (L-FDAA) to form diastereomers that were analyzed by reversed phase HPLC-MS. During the procedure the disulfide bridge was cleaved as well, allowing to assign also the cysteine stereochemistry. The elution order of β-OH Asp was established to be D -> L.[25] All amino acids were assigned to L configuration with Hyp being *trans*-4-hydroxy-L-proline, and Hya being L-*threo*-β-hydroxyaspartic acid (Figure S15).

The amount of SIP^+ released by *S. robusta* to signal its readiness for sexual reproduction was estimated by sampling the medium of the diatom culture and directly submitting it to UHPLC-MS. A *S. robusta* cell produces ≈150–400 amol SIP^+ within five days, which adds up to a low nanomolar range of SIP^+ produced by 20k cells cm^{-2} (final cell density) assuming stability of the pheromone over time.

Using the purified pheromone, we could also estimate the threshold concentration required to induce the production of the attraction pheromone in its mating partner. The activity of the pure compound to induce diproline was estimated in the low femtomolar range (Figure S16). This is substantially lower than the nanomolar concentration of diproline required to trigger the search behavior in *S. robusta.*[26] Given the fact that the cells produce SIP^+ continuously once they reach their sexual size threshold to signal readiness for mating, it becomes evident that a high sensitivity towards this pheromone is helping an economic synchronization. In contrast, diproline is only produced once the mating partner perceived the SIP^+ signal. Similarly sensitive pheromone systems are rarely reported, but Sumper et al. argue that perception of the green algal *Volvox*-pheromone, which is even more sensitive than that of SIP^+ might be supported by signal amplification within the extracellular matrix of the alga.[27] Because diatoms also build up a "phycosphere" of organic material, such an enrichment might be envisaged here as well.

It is remarkable that both hitherto elucidated diatom pheromones are peptides. While the structurally simple diketopiperazine derived from proline is the attractant, SIP^+ is a much more complex metabolite but also of peptidic nature. The structure of SIP^+ suggests a nonribosomal peptide synthetase (NRPS) to be involved in the biosynthesis. There are, however, very few reported NRPS in algae and especially in diatoms only one putative member of this enzyme class was detected by mining the available genomes.[28] We also know of no reported peptides with structures of similar complexity as SIP^+ in diatoms, suggesting that this compound opens up a new class of algal metabolites. Given its activity in lowest concentrations, the metabolite has the potential to synchronize entire algal-dominated communities.

In conclusion, starting from microgram quantities, a combination of HR-MS and NMR analyses combined with labeling experiments and chemical transformation led to the structure of the SIP^+ from the diatom *S. robusta.* The importance of ESI MS measured in negative ion mode should be emphasized. The compound is released by the algae continuously once they have reached a sexual size

threshold and become sexually active. The low effective concentrations guarantee that the resources required for the formation of the signal molecule are reduced to a minimum.

Acknowledgements

WV acknowledges partial financial support from project FWO G001521 N, BOF/GOA No. 01G01715 and infrastructure funded by EMBRC Belgium-FWO project GOH3817 N. GP acknowledges funding within the framework of the Germany's Excellence Initiative DFG-EXC 2051 Balance of the Microverse- Project-ID 390713860. Open Access funding enabled and organized by Projekt DEAL.

Conflict of Interest

The authors declare no conflict of interest.

Data Availability Statement

The data that support the findings of this study are available from the corresponding author upon reasonable request.

Keywords: Cell Cycle Arrest · Diatoms · Marine Biofilms · Peptide Sex Pheromone · Structure Elucidation

[1] W. M. Lewis, *Am. Nat.* **1984**, *123*, 73–80.
[2] A. Amato, *Int. J. Plant Reprod. Biol.* **2010**, *2*, 1–10.
[3] A. Poulíčková, D. G. Mann, *Diatoms: Fundamentals and Applications*, Wiley, Hoboken, **2019**, pp. 245–272.
[4] E. Scalco, A. Amato, M. I. Ferrante, M. Montresor, *Protoplasma* **2016**, *253*, 1421–1431.
[5] S. Basu, S. Patil, D. Mapleson, M. T. Russo, L. Vitale, C. Fevola, F. Maumus, R. Casotti, T. Mock, M. Caccamo, M. Montresor, R. Sanges, M. I. Ferrante, *New Phytol.* **2017**, *215*, 140–156.
[6] S. Sato, G. Beakes, M. Idei, T. Nagumo, D. G. Mann, *PLoS One* **2011**, *6*, e26923.
[7] V. A. Chepurnov, D. G. Mann, W. Vyverman, K. Sabbe, D. B. Danielidis, *J. Phycol.* **2002**, *38*, 1004–1019.
[8] C. M. Osuna-Cruz, G. Bilcke, E. Vancaester, S. De Decker, A. M. Bones, P. Winge, N. Poulsen, P. Bulankova, B. Verhelst, S. Audoor, D. Belisova, A. Pargana, M. Russo, F. Stock, E. Cirri, T. Brembu, G. Pohnert, G. Piganeau, M. I. Ferrante, T. Mock, L. Sterck, K. Sabbe, L. De Veylder, W. Vyverman, K. Vandepoele, *Nat. Commun.* **2020**, *11*, 3320.
[9] E. Cirri, S. De Decker, G. Bilcke, M. Werner, C. M. Osuna-Cruz, L. De Veylder, K. Vandepoele, O. Werz, W. Vyverman, G. Pohnert, *Front. Microbiol.* **2019**, *10*.
[10] J. Gillard, J. Frenkel, V. Devos, K. Sabbe, C. Paul, M. Rempt, D. Inzé, G. Pohnert, M. Vuylsteke, W. Vyverman, *Angew. Chem. Int. Ed.* **2013**, *52*, 854–857.
[11] S. Moeys, J. Frenkel, C. Lembke, J. T. F. Gillard, V. Devos, K. Van den Berge, B. Bouillon, M. J. J. Huysman, S. De Decker, J. Scharf, A. Bones, T. Brembu, P. Winge, K. Sabbe, M. Vuylsteke, L. Clement, L. De Veylder, G. Pohnert, W. Vyverman, *Sci. Rep.* **2016**, *6*, 19252.
[12] J. H. Bowie, C. S. Brinkworth, S. Dua, *Mass Spectrom. Rev.* **2002**, *21*, 87–107.
[13] P. Roepstorff, J. Fohlman, *Biomed. Mass Spectrom.* **1984**, *11*, 601.
[14] A. G. Harrison, A. B. Young, *J. Mass Spectrom.* **2005**, *40*, 1173–1186.
[15] D. Bilusich, J. H. Bowie, *Mass Spectrom. Rev.* **2009**, *28*, 20–34.
[16] D. Bilusich, V. M. Maselli, C. S. Brinkworth, T. Samguina, A. T. Lebedev, J. H. Bowie, *Rapid Commun. Mass Spectrom.* **2005**, *19*, 3063–3074.
[17] J. S. Martinez, G. P. Zhang, P. D. Holt, H.-T. Jung, C. J. Carrano, M. G. Haygood, A. Butler, *Science* **2000**, *287*, 1245–1247.
[18] A. W. Robertson, N. G. McCarville, L. W. MacIntyre, H. Correa, B. Haltli, D. H. Marchbank, R. G. Kerr, *J. Nat. Prod.* **2018**, *81*, 858–865.
[19] B. O. Petersen, E. Vinogradov, W. Kay, P. Würtz, N. T. Nyberg, J. Ø Duus, O. W. Sørensen, *Carbohydr. Res.* **2006**, *341*, 550–556.
[20] D. Sharma, K. Rajarathnam, *J. Biomol. NMR* **2000**, *18*, 165–171.
[21] T. Galica, N. Borbone, J. Mareš, A. Kust, A. Caso, G. Esposito, K. Saurav, J. Hájek, K. Řeháková, P. Urajová, V. Costantino, P. Hrouzek, H. Nojiri, *Appl. Environ. Microbiol.* **2021**, *87*, e03128–03120.
[22] K. F. Medzihradszky, Z. Darula, E. Perlson, M. Fainzilber, R. J. Chalkley, H. Ball, D. Greenbaum, M. Bogyo, D. R. Tyson, R. A. Bradshaw, A. L. Burlingame, *Mol. Cell. Proteomics* **2004**, *3*, 429–440.
[23] A. Plaza, G. Bifulco, M. Masullo, J. R. Lloyd, J. L. Keffer, P. L. Colin, J. N. Hooper, L. J. Bell, C. A. Bewley, *J. Org. Chem.* **2010**, *75*, 4344–4355.
[24] C. Kaufmann, M. Sauter, *J. Exp. Bot.* **2019**, *70*, 4267–4277.
[25] K. Fujii, Y. Ikai, T. Mayumi, H. Oka, M. Suzuki, K.-I. Harada, *Anal. Chem.* **1997**, *69*, 3346–3352.
[26] C. Lembke, D. Stettin, F. Speck, N. Ueberschaar, S. De Decker, W. Vyverman, G. Pohnert, *J. Chem. Ecol.* **2018**, *44*, 354–363.
[27] M. Sumper, E. Berg, S. Wenzl, K. Godl, *EMBO J.* **1993**, *12*, 831–836.
[28] E. O'Neill, *Mar. Drugs* **2020**, *18*, 19.

Manuscript received: June 7, 2023
Accepted manuscript online: August 21, 2023
Version of record online: September 14, 2023